Journal of Toxicology and Environmental Health, Part A: Current Issues
Publication details, including instructions for authors and subscription information:
http://www.tandfonline.com/loi/uteh20

Multiwalled Carbon Nanotube-Induced Gene Signatures in the Mouse Lung: Potential Predictive Value for Human Lung Cancer Risk and Prognosis

Nancy L. Guo [a b], Ying-Wooi Wan [a], James Denvir [a], Dale W. Porter [c], Maricica Pacurari [a], Michael G. Wolfarth [c], Vincent Castranova [a c] & Yong Qian [c]

[a] Mary Babb Randolph Cancer Center, West Virginia University, Morgantown, West Virginia, USA

[b] Department of Community Medicine, School of Medicine, West Virginia University, Morgantown, West Virginia, USA

[c] Pathology and Physiology Research Branch, Health Effects Laboratory Division, National Institute for Occupational Safety and Health, Morgantown, West Virginia, USA

Version of record first published: 14 Aug 2012.

To cite this article: Nancy L. Guo, Ying-Wooi Wan, James Denvir, Dale W. Porter, Maricica Pacurari, Michael G. Wolfarth, Vincent Castranova & Yong Qian (2012): Multiwalled Carbon Nanotube-Induced Gene Signatures in the Mouse Lung: Potential Predictive Value for Human Lung Cancer Risk and Prognosis, Journal of Toxicology and Environmental Health, Part A: Current Issues, 75:18, 1129-1153

To link to this article: http://dx.doi.org/10.1080/15287394.2012.699852

Journal of Toxicology and Environmental Health, Part A, 75:1129–1153, 2012

ISSN: 1528-7394 print / 1087-2620 online
DOI: 10.1080/15287394.2012.699852

Taylor & Francis
Taylor & Francis Group

MULTIWALLED CARBON NANOTUBE-INDUCED GENE SIGNATURES IN THE MOUSE LUNG: POTENTIAL PREDICTIVE VALUE FOR HUMAN LUNG CANCER RISK AND PROGNOSIS

Nancy L. Guo[1,2], Ying-Wooi Wan[1], James Denvir[1], Dale W. Porter[3], Maricica Pacurari[1], Michael G. Wolfarth[3], Vincent Castranova[1,3], Yong Qian[3]

[1]Mary Babb Randolph Cancer Center, West Virginia University, Morgantown, West Virginia, USA
[2]Department of Community Medicine, School of Medicine, West Virginia University, Morgantown, West Virginia, USA
[3]Pathology and Physiology Research Branch, Health Effects Laboratory Division, National Institute for Occupational Safety and Health, Morgantown, West Virginia, USA

Concerns over the potential for multiwalled carbon nanotubes (MWCNT) to induce lung carcinogenesis have emerged. This study sought to (1) identify gene expression signatures in the mouse lungs following pharyngeal aspiration of well-dispersed MWCNT and (2) determine if these genes were associated with human lung cancer risk and progression. Genome-wide mRNA expression profiles were analyzed in mouse lungs ($n = 160$) exposed to 0, 10, 20, 40, or 80 μg of MWCNT by pharyngeal aspiration at 1, 7, 28, and 56 d postexposure. By using pairwise statistical analysis of microarray (SAM) and linear modeling, 24 genes were selected, which have significant changes in at least two time points, have a more than 1.5-fold change at all doses, and are significant in the linear model for the dose or the interaction of time and dose. Additionally, a 38-gene set was identified as related to cancer from 330 genes differentially expressed at d 56 postexposure in functional pathway analysis. Using the expression profiles of the cancer-related gene set in 8 mice at d 56 postexposure to 10 μg of MWCNT, a nearest centroid classification accurately predicts human lung cancer survival with a significant hazard ratio in training set ($n = 256$) and test set ($n = 186$). Furthermore, both gene signatures were associated with human lung cancer risk ($n = 164$) with significant odds ratios. These results may lead to development of a surveillance approach for early detection of lung cancer and prognosis associated with MWCNT in the workplace.

Carbon nanotubes (CNT) are of great research interest due to their unique physicochemical properties and represent an important class of engineered nanomaterials. Three forms of CNT exist, depending on the number of the walls: single-walled carbon nanotubes (SWCNT), double-walled carbon nanotubes (DWCNT), and multiwalled carbon nanotubes (MWCNT) (Aschberger et al. 2010). SWCNT consist of a single graphene sheet, rolled up in the form of a cylinder with a diameter in the nanoscale and lengths ranging up to several micrometers. MWCNT consist of several stacked single-wall carbon nanotubes and exhibit diameters up to 100 nm and lengths up to several micrometers (Pacurari et al. 2010). MWCNT have been widely used in various applications, including supercapacitors, batteries, structural materials in automotive and aerospace industries, elec-

This study is supported by NIH/NLM R01LM009500 (PI: Guo) and NCRR P20RR16440 and Supplement (PD: Guo). The findings and conclusions in this report are those of the author(s) and do not necessarily represent the views of the National Institute for Occupational Safety and Health. Software license and training for Ingenuity Pathway Analysis and Pathway Studio is supported by NIH/NCRR P2016477.

Address correspondence to Yong Qian, Pathology and Physiology Research Branch, Health Effects Laboratory Division, National Institute for Occupational Safety and Health, Morgantown, WV 26505, USA. E-mail: yaq2@cdc.gov

tronics, pharmaceutics, bioengineering, medical devices, and biomedicine (Pacurari et al. 2010; Zhao and Castranova 2011).

Concerns over MWCNT-induced potential health hazards have been raised due to their analogous physical properties to asbestos fibers, such as high aspect ratio (length/diameter), nanoscale diameter, micrometer length, fiber-like shape, and durability (Donaldson et al. 2006; Kobayashi et al. 2010; Muller et al. 2005; Tabet et al. 2009). Three properties of MWCNT might lead to pathogenicity in humans: (1) MWCNT are nanosized, so they could deposit in the deep lung and pose more toxicity than large sized particles; (2) MWCNT are long, thin, fibrous-like structures, which may exert asbestos-like pathogenic effects; and (3) MWCNT are resistant to high temperature and acid treatment, so are considered durable (Aschberger et al. 2010; Donaldson et al. 2006). For in vivo assessment of MWCNT, pulmonary toxicity was conducted using instillation, aspiration, and inhalation techniques. Several animal studies demonstrated that exposure to MWCNT induces inflammatory granulomas and substantial interstitial lung fibrosis in the lungs (Lam et al. 2004; Muller et al. 2005; Porter et al. 2010; Shvedova et al. 2005). Animal studies using intraperitoneal (ip) exposure also showed that MWCNT induced inflammatory granulomas and mesothelioma to a degree similar to asbestos fibers (Donaldson et al. 2006; Poland et al. 2008; Takita et al. 1986). Thus, MWCNT may pose a carcinogenic risk similar to asbestos fibers.

In vitro studies indicate that MWCNT are genotoxic, which may indicate carcinogenic potential of MWCNT. Exposure to MWCNT was shown to induce DNA damage and increase mutation frequency in both mouse embryonic cells and A549 type II epithelial cells (Karlsson et al. 2008; Tabet et al. 2009; Zhu et al. 2007). Recently, Sargent et al. (2011) found that MWCNT exposure induces mitotic abnormality with one rather than two mitotic spindle poles, which was proposed as the mechanism responsible for the disruption of cell division by MWCNT. It was also demonstrated that MWCNT-induced mesothelioma is accompanied by homozygous deletion of Cdkn2a/2b tumor suppressor genes, similar to mesotheliomas induced by asbestos (Nagai et al. 2011). Moreover, Muller et al. (2008) demonstrated that MWCNT exposure increases genotoxic potential both in vivo and in vitro.

Recently, our group conducted an in vivo dose-response and time-course study of MWCNT exposure in mice in order to investigate the ability of MWCNT to induce pulmonary inflammation, damage, and fibrosis (Porter et al. 2010). Mice were exposed to 0, 10, 20, 40, or 80 μg of MWCNT by pharyngeal aspiration. At 1, 7, 28, and 56 d postexposure, MWCNT-induced pulmonary responses were evaluated. The results demonstrate that pulmonary inflammation and damage were dose dependent, appeared 1 d postexposure, and peaked 7 d postexposure. In contrast, morphometric analysis of lung tissues from the study by Mercer et al. (2011) indicated that MWCNT-induced interstitial fibrosis increased significantly at d 28 and progressed through 56 d postexposure. These results suggest that MWCNT exposure rapidly produces significant pulmonary inflammation, damage, and fibrosis.

Fibrosis is a pulmonary fibrotic scarring and may be a precursor to lung cancer. Yu et al. (2008) found an association between elevated lung cancer risk and lung scarring; furthermore, they found that pulmonary scarring and lung cancer occurred in the same lung regions and extended over time, indicating that lung cancer could originate from lung scarring. Indeed, in a review of lung cancer patients over a 21-yr period, it was demonstrated that 45% of all peripheral lung cancers originated from a lung scar (Auerbach et al. 1979). A possible association between lung cancer and fibrosis was revealed by a study with computed tomographic (CT) scans and pathologic specimen analysis, in which 47 out of 57 histologically proven lung cancers had pulmonary fibrosis (Sakai et al. 2003). The chronic pulmonary scarring in the etiology of lung cancer was also observed in crystalline silica-exposed patients and tuberculosis patients. Several clinical studies found that the increased risk of lung cancer among patients with silicosis, a progressive lung

fibrosis, might be an effect of the lung fibrosis rather than a direct effect of silica exposure (Peretz et al. 2006); furthermore, tuberculosis-induced lung fibrosis was associated with an increased lung cancer risk (Shiels et al. 2011).

Several similar biological and pathological characteristics were found in both lung fibrosis and lung cancer, including genetic alterations, uncontrolled proliferation, and tissue invasion (MacKinnon et al. 2010). Interestingly, it was discovered that the expression of TGF-beta, a well-established cancer biomarker, is elevated in asbestos-induced fibrosis as determined by immunohistochemical analysis (Jagirdar et al. 1997). TGF-beta is a ubiquitous and essential regulator of cellular proliferation, differentiation, migration, cell survival, and angiogenesis (Elliott and Blobe 2005). An alteration of TGF-beta expression was associated with increased human cancer incidence, including lung cancer. A rise in TGF-beta expression in asbestos-induced fibrosis suggests that pulmonary fibrosis may increase the risk of lung carcinogenesis.

Although more research is needed for the assessment of the clinical outcome of lung fibrosis, Vancheri et al. (2010) suggested that the abnormal fibroblast proliferation observed in pulmonary fibrosis may be associated with the carcinogenesis of the lung. The current study was designed to follow up our previous investigation of MWCNT-induced pulmonary inflammation, damage, and fibrosis in the mouse model. The aim of this study was to identify MWCNT-induced gene expression changes in the MWCNT-exposed mouse lung tissues collected from a previous study by Porter et al. (2010) and determine whether similar gene expression profiles in humans were associated with the risk for lung cancer development and progression.

In vivo and in vitro gene expression signatures associated with specific histopathological phenotypes could be identified from toxicogenomic data (Amin et al. 2004; Hamadeh et al. 2002 2004; Luhe et al. 2003; Paules 2003; Powell et al. 2006) to predict human health ramifications based on similarities of gene expression profiles for risk assessment (Amin et al. 2004; Bushel et al. 2007). Specifically, in the study by Bushel et al. (2007), blood gene expression signatures identified from acetaminophen (APAP)-exposed rats could separate APAP-intoxicated patients from unexposed controls, indicating that gene expression data from peripheral blood cells can provide valuable information about environmental disease well before liver damage is detected by classical parameters. The unique advantage of such studies is the ability to detect toxic injury at the molecular level and to identify the molecular events that lead to organ injury long before the clinical symptoms occur. Similarly, the current study sought to identify MWCNT-induced gene expression patterns in an animal model and determine if similar gene expression patterns in humans are associated with the risk for lung cancer initiation and/or progression. The finding of an association would justify further long-term studies to determine the temporal association between MWCNT-induced gene alterations and the development of precancerous lesions and/or tumors in the mouse lung.

MATERIALS AND METHODS

MWCNT

MWCNT used in this study were a gift from Mitsui & Company (MWCNT-7, lot 05072001K28). The characterization of MWCNT has been published (Porter et al. 2010). Briefly, the bulk MWCNT exhibit a distinctive crystalline structure with the number of walls ranging from 20 to 50 walls. Overall, MWCNT trace metal contamination was 0.78%, including sodium (0.41%) and iron (0.32%), with no other metals present above 0.02%. Transmission electron microscopy (TEM) micrographs of MWCNT dispersed in dispersion medium (DM) demonstrated that DM promotes significant dispersion of MWCNT. The quantitative analysis of TEM micrographs revealed that the median length of this MWCNT sample was 3.86 μm (GSD 1.94) and the count mean width was 49 ± 13.4 (SD) nm. The zeta potential of the MWCNT in the DM was determined to be –11 mV.

Animals

Male C57BL/6J mice (7 wk old, 20 g on average) were obtained from Jackson Laboratories (Bar Harbor, ME). Since male mice fight and injure each other if caged together, individual mice were housed one per cage in polycarbonate isolator ventilated cages, which were provided HEPA-filtered air, with fluorescent lighting from 0700 to 1900 h. Autoclaved Alpha-Dri virgin cellulose chips and hardwood Beta-chips were used as bedding. Mice were monitored to be free of endogenous viral pathogens, parasites, mycoplasms, *Helicobacter,* and CAR *Bacillus*. Mice were maintained on Harlan Teklad Rodent Diet 7913 (Indianapolis, IN), and tap water was provided ad libitum. Animals were allowed to acclimate for at least 5 d before use. All animals used in this study were housed in an AAALAC-accredited, specific-pathogen-free, environmentally controlled facility.

MWCNT Pharyngeal Aspiration Exposure

Suspensions of MWCNT were prepared in DM as previously described by Porter et al. (2008). Each treatment group consisted of eight mice. Mice were anesthetized with isoflurane (Abbott Laboratories, North Chicago, IL). When fully anesthetized, a mouse was positioned with its back against a slant board and suspended by the incisor teeth using a rubber band. The mouth was opened, and the tongue gently pulled aside from the oral cavity. A 50-μl aliquot of sample was pipetted at the base of the tongue, and the tongue was restrained until at least 2 deep breaths were completed (but for not longer than 15 s). Following release of the tongue, the mouse was lifted off the board, placed on its left side, and monitored for recovery from anaesthesia. Mice received either DM (vehicle control), 10, 20, 40, or 80 μg MWCNT.

RNA Extraction

Total RNA was extracted from the frozen mouse lung tissue sample (–80°C) in RNAlater using the RNeasy Fibrous Tissue Mini Kit according to the manufacturer's protocol (Qiagen, USA). Total RNA was eluted in RNase-free water and stored at −80°C until further analysis. The quality and the concentration of each RNA sample were determined using a Nanodrop-1000 spectrophotometer (NanoDrop Tech, Germany).

Microarray Expression Profiling

Extracted RNA was analyzed for expression profiling using Agilent Mouse Whole Genome Arrays (Agilent, Santa Clara, CA). A universal reference design was employed, using Stratagene Universal Mouse Reference RNA, catalogue number 740100 (Agilent), as the reference RNA. Total RNA quality was determined on an Agilent 2100 bioanalyzer, with all samples having RNA integrity numbers (RIN) greater than 8. Total RNA (250 ng) was used for labeling using the QuickAmp labeling kit (Agilent). RNA extracted from each mouse was labeled with cyanine (Cy)-3-CTP (PerkinElmer, Waltham, MA), and reference RNA with (Cy)-5-CTP. Following purification of labeled cRNAs, 825 ng of Cy3- and Cy5-labeled cRNAs were combined and hybridized for 17 h at 65°C in an Agilent hybridization oven. Microarrays were then washed and scanned using an Agilent DNA microarray scanner.

Microarray Data Preprocessing and Filtering

Data were exported from the scanner using Feature Extraction v10 as tab-delimited text files after background subtraction, log transform, and lowess normalization and reported as log or relative expression of sample compared to universal reference. Data were read from each file into R using a custom script (source codes are available upon request). For each array, values for control spots, spots that were saturated on either channel, spots that were reported by Feature Extraction as nonuniform outliers on either channel, and spots that were not well above background on at least one channel were considered unreliable and/or uninformative and were replaced by "NA." Values were collated into a single table,

and probes for which fewer than 10 present values were available were removed. For probes spotted multiple times on the array, values were averaged across replicate probes. The resulting table is available as a series matrix file in the NCBI Gene Expression Omnibus repository with accession number GSE29042.

Missing data were imputed using the K-means nearest neighbor algorithm as implemented by the *impute.knn* function in the impute *R* package from *Bioconductor* (www.bioconductor.org). For each dose and each time point, a set of differentially expressed genes was identified by performing a two-class unpaired significance analysis of microarrays (SAM) between the treated samples and the dose-zero samples from the corresponding time point, using the *Bioconductor* package. A threshold delta value was chosen to produce a false discovery rate of 1% using the *findDelta* function from the same package. The list of probes called significant was subsequently filtered by restricting to those probes that were at least 1.5-fold up- or downregulated (fold changes were computed from the data before imputation of missing values). This stage of the analysis was referred to as the "pairwise-SAM analysis."

Identification of MWCNT-Induced Gene Expression Signatures

For each time point a list was constructed of genes that were statistically significant by pairwise-SAM at one or more doses, and that had at least 1.5-fold changes at all four treatment doses. Each of these time-point-associated gene sets was imported into Ingenuity Pathway Analysis (IPA: Ingenuity Systems, Redwood City, CA) and a Core Analysis was performed on each one. The "diseases and disorders" functions and the canonical pathways identified in each core analysis were examined. In either case, a Benjamini–Hochberg adjusted p value with a threshold of .05 was used to assess significance.

Additionally, a linear model was fit to the data, modeling the log expression of each gene in turn as a function of time, dose, and the interaction of time with dose. The t-statistic associated with the dose and interaction parameters was moderated following the SAM algorithm and a threshold was set to control for a false discovery rate of 0.1%, generating a list of genes whose expression values were significantly dependent on dose and a list of genes whose expression values were significantly dependent on dose in a time-dependent fashion.

In order to generate a list of probes that were consistently differentially expressed across multiple conditions, probes were selected that belonged to two or more of the lists of probes generated for each time point, and then this list was intersected with the union of the two lists of probes from the linear model. These were considered to be probes whose expression is significantly changed for a substantial portion of the entire time course of the experiment and that significantly show a dose-dependent expression variation. This collection of probes was termed the "consistently differentially expressed set."

Second, since it has been postulated that exposure to MWCNT may induce a chronic carcinogenic response, a bioinformatic functional analysis was performed on the genes differentially expressed at the 56-d time point. A core analysis was performed on this list of genes with Ingenuity Pathway Analysis (IPA) software (Ingenuity Systems, Redwood City, CA). Genes identified by the core analysis as being related to cancer were selected. These cancer-related genes were exported to a new list, and then connections among these genes were built using all available relationships provided by IPA. The largest subset of genes with known connectivity within this set was selected and termed as the "56-day cancer-related gene set."

Patient Samples and Microarray Profiles

Microarray gene expression data from two published studies were used in the analyses. The first study cohort contains 442 lung adenocarcinoma patient samples obtained from the Director's Challenge Study (Director's Challenge Consortium for the Molecular Classification of Lung et al. 2008). This study

cohort is composed of four data sets (UM, HLM, DFCI: University of Michigan, H. Lee Moffitt Cancer Center, Memorial Sloan-Kettering Cancer Center, and Dana–Farber Cancer Institute) contributed by six institutions. The raw microarray data are available from the caArray website (https://array.nci.nih.gov/caarray/project/details.action?project.id=182). In our lung cancer prognosis analyses, a training set was formed by combining UM and HLM cohorts, and the test set was the combination of MSK and DFCI cohorts. Table 1 gives a brief summary on the patient characteristics of the two datasets. The second study cohort contains 164 airway epithelial cell samples collected from normal individuals, small cell and non-small cell lung cancer patients (Spira et al. 2007). This cohort was randomly partitioned into training set ($n = 77$), Test set 1 ($n = 52$), and Test set 2 ($n = 35$). A summary of patients' clinical information in the second study cohort is listed in Table 2. Genome-wide expression profiles of patients in both data sets were measured with Affymetrix HG-U133A. Data used in this study were quantile-normalized and $\log_2$-transformed with dChip (Wheeler et al. 2008).

TABLE 1. Patient Characteristics From Director's Challenge study (Director's Challenge Consortium for the Molecular Classification of Lung et al. 2008)

	UM and HLM (Training, $n = 256$)	MSK and DFCI (Test, $n = 186$)
Age, mean (SD)	65 (10)	63 (10)
Gender (% male)	55%	44%
Tumor stage		
Stage I	61% (157/256)	64% (119/186)
Stage II	19% (49/256)	25% (46/186)
Stage III	18% (47/256)	11 % (21/186)
Stage IV	—	—
Unknown	1% (3/256)	—

Computational Methods for Diagnostic and Prognostic Classifications

Nearest shrunken centroid classification The nearest shrunken centroid method was employed in predicting lung cancer progression based on the MWCNT-induced gene expression signatures in the treated animal group. This algorithm categorizes an unknown instance to the class whose centroid is closest to it. It considers the centroid of the cluster as a representative of the class. The learned distance function is used to determine the closest centroid (Elick et al. 2006). For cases involving two classes, the nearest centroid algorithm is linear and implicitly encodes a threshold hyperplane that separates the two classes (Levner 2005).

Specifically, the arithmetic mean of a class C_j represents the prototype pattern for the class (i.e., the average expression of each signature gene in the training centroid of the treated animal group) and is denoted by Eq. (1):

$$\mu_{C_j} = \frac{1}{|C_j|}\sum_{x_i \in C_j} x_i \qquad (1)$$

TABLE 2. Patient Characteristics From Spira et al. (2007)

	Training ($n = 77$)	Test 1 ($n = 52$)	Test 2 ($n = 35$)
Age, mean (SD)	57 (14)	55 (16)	64 (11)
Gender (% male)	78%	75%	69%
Lung cancer histology			
Small-cell	15% (6/40)	25% (5/20)	17% (3/18)
Non-small-cell	83% (33/40)	75% (15/20)	78% (14/18)
Unknown	2% (1/40)	—	5% (1/18)
Small-cell tumor stage			
Limited	3 (3/6)	4	2
Extensive	3 (3/6)	1	1
NSCLC tumor stage			
Stage I	30% (10/33)	7% (1/15)	14% (2/14)
Stage II	—	13% (2/15)	—
Stage III	30% (10/33)	47% (7/15)	36% (5/14)
Stage IV	39% (13/33)	33% (5/15)	29% (4/14)
Unknown	—	—	21% (3/14)

where x_i represents the training samples that belong to the class C_j.. Using this algorithm, a class label of an unknown instance x is predicted as Eq. (2):

$$C(x) = \arg\min_{C_j} d(\mu_{C_j}, x) \quad (2)$$

where *d(x,y)* denotes the distance function (Levner 2005).

The distance function measures the strictness of dependence between the two vectors (Strickert 2007). In this study, Pearson's correlation was used as the distance measure in nearest centroid classification. Pearson's correlation provides the degree of linear dependence of vectors x and w by Eq. (3):

$$R(x, w) = \frac{\sum_{i=1}^{d} (x_i - \mu x)\cdot(w_i - \mu w)}{\sqrt{\sum_{i=1}^{d} (x_i - \mu x)^2 \cdot \sqrt{\sum_{i=1}^{d} (w_i - \mu w)^2}}} \quad (3)$$

where μx and μw are the respective means of the vectors x (gene expression signature in the training centroid) and w (gene expression signature in a test sample). The equation is standardized by the multiplication of the standard deviations of the vectors after subtracting their respective means. This causes the Pearson's correlation to be invariant (Strickert 2007).

Random committee was used to classify lung cancer patients from normal individuals using the "56-day cancer-related gene set." Random committee is a meta-learning algorithm that builds an ensemble of randomization-based classifiers and averages their predictions as the final result. Each base classifier constructed in the ensemble is learned on the same data but uses a difference random number seed. In this study, random forests were used as the base classifiers for the Random committee algorithm implemented in software WEKA 3.6 (Witten 2005).

RIPPER was employed in the classification of lung cancer patients from normal individuals using the "consistently differently expressed gene set." RIPPER is a propositional rule learning algorithm proposed by Cohen (1995) with improvement over original incremental reduced error pruning (IREP). In this new algorithm, after an initial rule set is learned from IREP, the rule set is further pruned repeatedly based on a different metric and stopping condition on randomized data. The repeated pruning stops when the rule set learned from IREP is refined into a rule set with optimized size and performance. JRip learner was employed in the analysis with software WEKA 3.6 (Witten 2005).

RESULTS

Identification of MWCNT-Induced Gene Expression Signatures

Genome-wide expression profiles were quantified on the lung tissues collected from 160 mice at 1, 7, 28 and 56 d after MWCNT aspiration. For each time point, a group of mice ($n = 8$) was exposed to 0 (control), 10, 20, 40, or 80 μg of well-dispersed MWCNT particles, respectively. Genes were selected based on the pairwise-SAM analysis and linear modeling, selecting genes that showed significant changes in at least two time points and that had a more than 1.5-fold change at all doses and were significant in the linear model for the dose or the interaction of time and dose. The consistently differentially expressed gene set consists of 26 probes representing 24 unique genes. Table 3 shows these genes along with the time points at which they were determined to be significantly differentially expressed. The expression of these 24 genes also exhibited a significant linear relationship in response to treatment dose, or a linear dose response over the time course. All probes in this list showed increased expression at all positive doses relative to the control at these time points.

The 330 genes that were differentially expressed at 56 d were examined in order to assess the possible chronic carcinogenic effect of MWCNT exposure. From these 330 genes, IPA identified 91 that were associated with cancer. Connections were found between 41 of these genes, with 38 of the 41 forming a larger network and the three remaining genes forming a small, disconnected set (Figure 1A). The 38 in the major network, shown in Table 4, form our "56-day cancer-related gene set."

TABLE 3. The Consistently Differentially Expressed Gene Set, Showing the Time Points at Which They Were Determined to Be Significantly Regulated

Probe ID in mouse genome	Gene name	MWCNT treated animal groups				Included in human lung cancer studies
		Day 1	Day 7	Day 28	Day 56	
A_51_P309307	BCL2L15	☑	☑	☐	☐	
A_52_P18116	CCL24	☑	☑	☐	☐	✓
A_51_P185660	CCL9	☑	☑	☐	☑	
A_51_P112966	CH25H	☑	☑	☑	☑	✓
A_51_P383032	CLEC4D	☑	☐	☐	☑	
A_52_P218058	CLEC5A	☑	☑	☑	☑	
A_51_P363187	CXCL1	☑	☐	☑	☑	✓
A_52_P232813	CXCL3	☑	☐	☑	☐	✓
A_52_P295432	CXCL5	☑	☐	☐	☑	✓
A_51_P173043	EGR2	☑	☑	☐	☐	✓
A_51_P130095	FCGR2B	☑	☑	☐	☐	✓
A_51_P438967	GPNMB	☐	☑	☑	☑	
A_51_P217218	IL6	☑	☑	☐	☑	✓
A_51_P241457	LILRB4	☑	☑	☐	☐	✓
A_51_P404846	MSR1	☑	☑	☐	☐	✓
A_52_P607128	MSR1	☑	☑	☐	☐	✓
A_51_P512379	NAP109359-1	☑	☑	☐	☐	
A_52_P625940	NOXO1	☑	☑	☐	☐	
A_52_P700056	OTTMUSG00000000971	☑	☑	☑	☑	
A_51_P260683	RGS1	☑	☑	☐	☑	✓
A_51_P249286	RGS16	☑	☐	☑	☐	✓
A_51_P337308	SAA3	☑	☑	☑	☐	✓
A_51_P358765	SPP1	☑	☑	☑	☑	✓
A_52_P87713	TIMP1	☑	☑	☐	☐	✓
A_52_P210511	TNFRSF9	☑	☑	☐	☐	✓
A_52_P75441	TNFRSF9	☑	☑	☐	☐	✓

Note. The genes MSR1 and TNFRSF9 are represented by multiple distinct probes. All probes marked as having significant changes have increased expression levels at all doses. A total of 16 genes (with 18 probes) were included in human lung cancer studies.

Genes in both signatures were retrieved from the human microarray data. Eighteen out of the 24 consistently differentially expressed genes were matched in human genome using gene symbols. Next, 2 of the 18 matched genes were removed from the study as they had missing values in more than half of the cancer patient samples, resulting in a final list of 16 genes (with 18 probes; Table 3). Similarly, after matching to the human microarray platform and removing genes with missing values in most cancer patient samples, 35 of the 38 genes in the "56-day cancer-related gene set" were used for further analysis (Table 4). Furthermore, there was exploration of whether the 16- and 35-gene signatures could predict human lung cancer risk and prognosis.

Predicting Lung Cancer Progression and Metastasis Using the 35-Gene Signature

Experiments were conducted to determine whether gene expression signature in the mouse lung post MWCNT exposure is associated with the risk for tumor progression and metastasis in a human lung cancer cohort. The 35-gene signature is composed of cancer-related genes that were differentially expressed at d 56 after exposure in the mouse lung. The observed gene expression patterns in MWCNT-treated mice were used to predict human lung cancer clinical outcome. A nearest shrunken centroid classification scheme was employed in the prediction using the correlation between a patient's gene expression profiles and the expression centroid of the

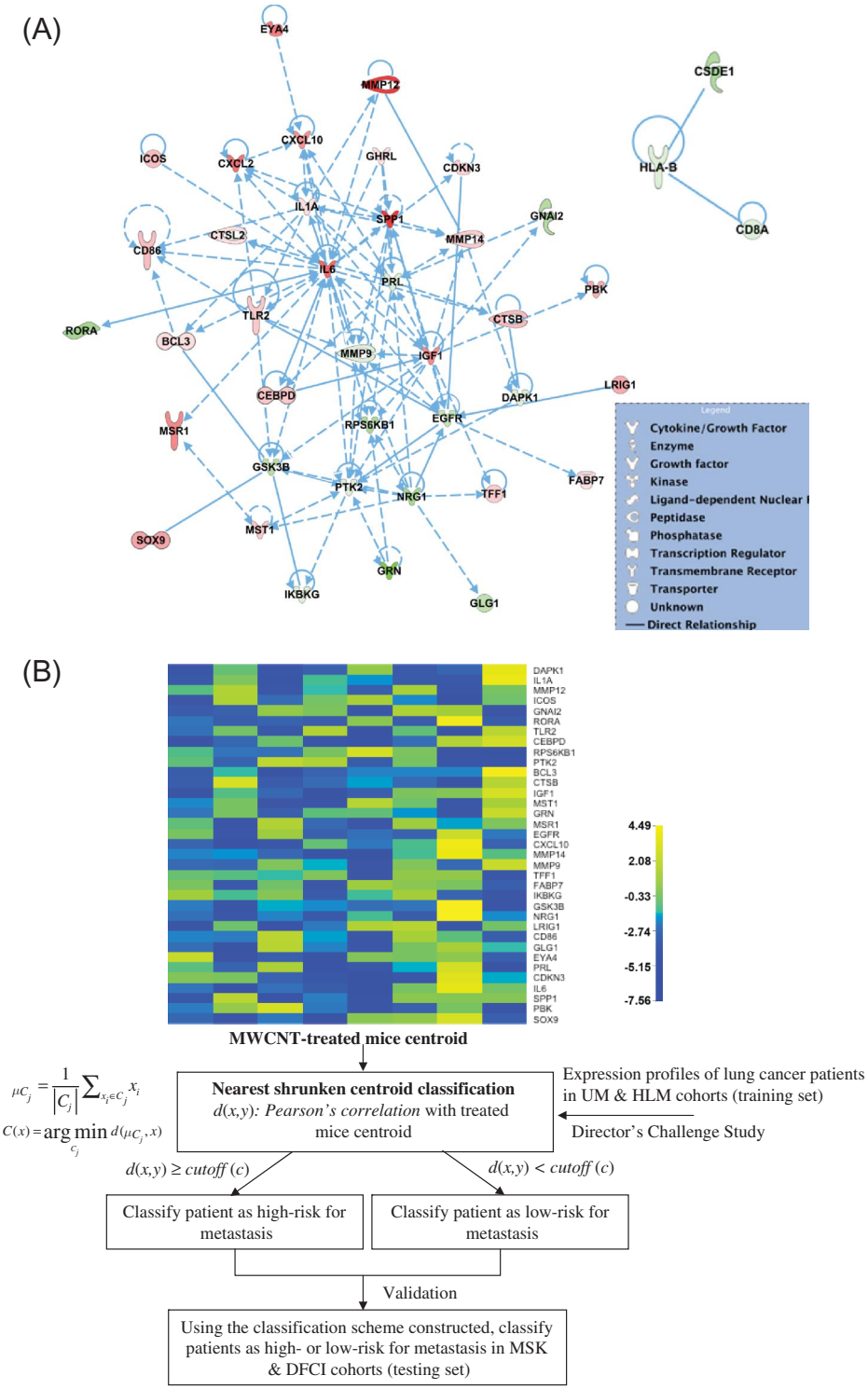

FIGURE 1. The risk assessment scheme of lung cancer progression in humans based on the identified gene expression signature in MWCNT-treated mice. (A) Molecular network generated from genes associated with cancer which are differentially expressed at d 56 in MWCNT-treated mice. Shading denotes degree of differential expression with a dose of 40 μg, with red denoting upregulated genes and green denoting downregulated genes. (B) Nearest shrunken centroid classification method stratified a patient into a high- or low-risk group for metastasis based on Pearson correlation between the gene expression profiles in the patient tumor and those in the treated mice centroid for a particular dose on d 56 after MWCNT aspiration. The cutoff for patient stratification was identified from the training cohort (UM and HLM) and validated in the test cohort (MSK and DFCI) from the Director's Challenge Study (Director's Challenge Consortium for the Molecular Classification of Lung et al. 2008) (color figure available online).

TABLE 4. The 56-Day Cancer-Related Gene Set

Gene symbol	Location	Family	Included in human lung cancer studies
BCL3	Nucleus	Transcription regulator	✓
CD86	Plasma membrane	Transmembrane receptor	✓
CDKN3	Nucleus	Phosphatase	✓
CEBPD	Nucleus	Transcription regulator	✓
CTSB	Cytoplasm	Peptidase	✓
CTSL2	Cytoplasm	Peptidase	
CXCL10	Extracellular space	Cytokine	✓
CXCL2	Extracellular space	Cytokine	
DAPK1	Cytoplasm	Kinase	✓
EGFR	Plasma membrane	Kinase	✓
EYA4	Cytoplasm	Phosphatase	✓
FABP7	Cytoplasm	Transporter	✓
GHRL	Extracellular space	Growth factor	
GLG1	Cytoplasm	Other	✓
GNAI2	Plasma membrane	Enzyme	✓
GRN	Extracellular space	Growth factor	✓
GSK3B	Nucleus	Kinase	✓
ICOS	Plasma membrane	Other	✓
IGF1	Extracellular space	Growth factor	✓
IKBKG	Nucleus	Kinase	✓
IL1A	Extracellular space	Cytokine	✓
IL6	Extracellular space	Cytokine	✓
LRIG1	Extracellular space	Other	✓
MMP12	Extracellular space	Peptidase	✓
MMP14	Extracellular space	Peptidase	✓
MMP9	Extracellular space	Peptidase	✓
MSR1	Plasma membrane	Transmembrane receptor	✓
MST1	Extracellular space	Growth factor	✓
NRG1	Extracellular space	Growth factor	✓
PBK	Cytoplasm	Kinase	✓
PRL	Extracellular space	Cytokine	✓
PTK2	Cytoplasm	Kinase	✓
RORA	Nucleus	Ligand-dependent nuclear receptor	✓
RPS6KB1	Cytoplasm	Kinase	✓
SOX9	Nucleus	Transcription regulator	✓
SPP1	Extracellular space	Cytokine	✓
TFF1	Extracellular space	Other	✓
TLR2	Plasma membrane	Transmembrane receptor	✓

Note. A total of 35 genes were used for human lung cancer studies.

same genes in MWCNT-treated mouse lungs (Figure 1B). Specifically, the risk for lung cancer progression and metastasis associated with the 35-gene signature at different doses (including 10 μg, 20 μg, 40 μg, and 80 μg) was evaluated, respectively.

Lung adenocarcinoma patients from the Director's Challenge study (Director's Challenge Consortium for the Molecular Classification of Lung et al. 2008) were separated into training (UM and HLM cohorts, $n = 256$) and test (MSK and DFCI cohorts, $n = 186$) sets. In the training cohort, the correlation coefficient between the 35-gene centroid in MWCNT-treated mice and the 35-gene expression profiles in each lung cancer patient was computed. This correlation indicates the level of similarity between the gene expression profiles in lung adenocarcinoma patients and those in the MWCNT-exposed mice. Based on the distribution of the correlation coefficients in the training cohort, a cutoff value was identified to stratify patients into two risk groups. A patients was identified to be at high risk for metastasis if the 35-gene expression profiles in this patient were similar

to those in the MWCNT-exposed mice (with a correlation coefficient greater than or equal to the cutoff value); otherwise, the patient was considered at low risk for metastasis. This patient stratification scheme was then validated by the independent test set (Figure 1B).

Figure 1B illustrates the 35-gene expression centroid in 8 mice treated with 10 μg MWCNT at d 56 after the aspiration. Using this gene expression centroid, a correlation coefficient of 0.182 was defined as the cutoff to stratify patients into a high- or low-risk group for lung cancer progression and metastasis (Figure 2A). Based on the level of similarity to the 35-gene expression profiles in the MWCNT-treated mice, cancer patients with a more similar gene expression pattern had significantly higher risk of death from lung cancer in both training and test sets (*HR* = 2.19, 95% CI: [1.43, 3.34] in training set; *HR* = 1.99, 95% CI: [1.16, 3.4] in the test set; Figure 2B). The expression-defined risk groups had significantly distinct disease-specific survival after surgery in both training and test sets (Figure 2B). The 35-gene MWCNT signature accurately predicted 3-yr survival in lung adenocarcinoma patients with an overall accuracy of 64% in the training set and 70% in the test set, predictions that were significantly more accurate compared with random predictions (Figure 2C). Furthermore, the 35-gene signature could further stratify stage 1 lung adenocarcinoma into different prognostic groups with

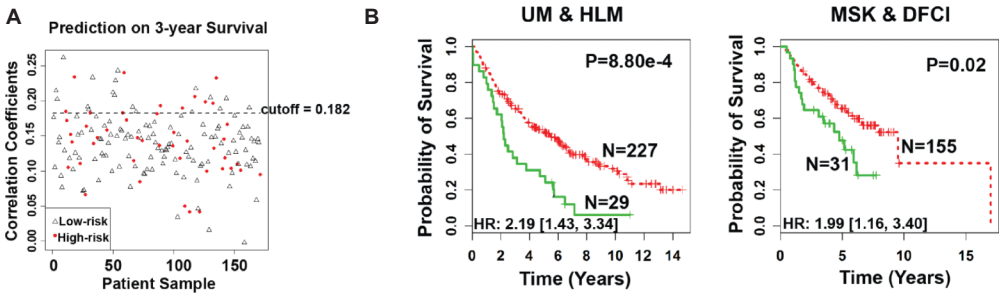

C

3-year Survival Prediction	Training (UM&HLM)	Testing (MSK&DFCI)
Sensitivity	18.95%	24.44%
Specificity	92.76%	85.71%
Overall Accuracy	64.37%	69.59%
***P*-value**	6.19e-4	1.12e-4

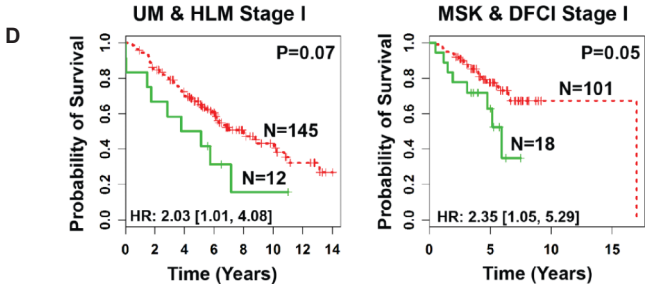

FIGURE 2. The risk assessment model of lung cancer progression based on the 35-gene MWCNT signature. The 35-gene centroid in 8 mice treated with 10 μg of MWCNT at 56 d after exposure was used to predict lung cancer progression and metastasis in a set of human lung adenocarcinoma patients. (A) Patients were classified into a high- or low-risk group for metastasis based on the Pearson's correlation to the treated mice centroid with a cutoff value of 0.182. Three-year disease-specific survival was used to define risk groups for metastasis in lung adenocarcinoma patients. (B) In Kaplan–Meier analysis, the 35-gene MWCNT signature stratified patients into two groups with significantly distinct survival outcome in both training (log-rank $P < 8.8e\text{-}4$; UM and HLM) and test (log-rank $P < 0.02$; MSK and DFCI) cohorts. Red curve: low-risk (good-prognosis) patient group; green curve: high-risk (poor-prognosis) patient group. (C) The performance of the 35-gene MWCNT signature in predicting 3-yr survival. (D) The 35-gene MWCNT further stratified stage I lung adenocarcinoma into distinct risk groups with significantly different hazard ratios of death from lung cancer (color figure available online).

distinct disease-specific survival (Figure 2D). For stage 1 lung adenocarcinoma patients, tumors with gene expression patterns more similar to those in the mice treated with 10 μg of MWCNT had significantly greater potential of cancer progression and metastasis with a much shorter period of survival compared with the tumors without this MWCNT-induced gene signature (*HR* = 2.03, 95% CI: [1.01, 4.08] in training set; *HR* = 2.35, 95% CI: [1.05, 5.29] in the test set; Figure 2D). These results indicate that human lung tumors with the MWCNT-induced gene expression patterns were more likely to be aggressive and had shorter overall survival compared with those with unexposed gene expression patterns. Notably, the specificity of the 35-gene MWCNT signature was greater than 86% in both training and test sets (Figure 2C), indicating that the gene signature from the mouse MWCNT exposure study had an association with lung cancer progression in patients with adenocarcinoma.

Similarly, the risk of lung cancer progression associated with the 35-gene MWCNT signature was evaluated for dose 20, 40, or 80 μg, respectively (Figure 3). In the training set, the 35-gene signature gave significant hazard ratios for all treatment doses. In the test set, the corresponding models had significant hazard ratios for lower doses (10 and 20 μg), but not for the higher doses (40 and 80 μg; Figure 3). These results indicate that the 35-gene signature in the mouse lung treated with low doses of MWCNT most accurately predicted the risk for tumor progression and metastasis in human lung adenocarcinoma patients. The 35-gene expression profiles in the mouse lungs treated with higher doses did not generate accurate risk assessment of tumor progression, due to the fact that a large number of genes were significantly changed in dose 80 μg at 56 d postexposure (with a total of 1214 genes; fold change >1.5, FDR < 1%, SAM). Therefore, using only 35 genes cannot accurately represent the overall gene expression changes induced by higher doses of MWCNT exposure in the risk assessment.

Implications in Early Detection of Human Lung Cancer

After establishing the relevance of MWCNT-induced gene signature in predicting human lung cancer progression, we explored whether these signatures could be used for assessment of human lung cancer risk. The cohort from Spira et al. (2007) contained small-cell lung cancers, non-small-cell lung cancers, and normal lung tissues. This cohort was randomly partitioned into a training set ($n = 77$) and two independent test sets, Test set 1 ($n = 52$) and Test set 2 ($n = 35$). Patient characteristics in the training and testing sets are summarized in Table 2. In the risk assessment of human lung cancer initiation, the 35- and 16-gene signatures were used

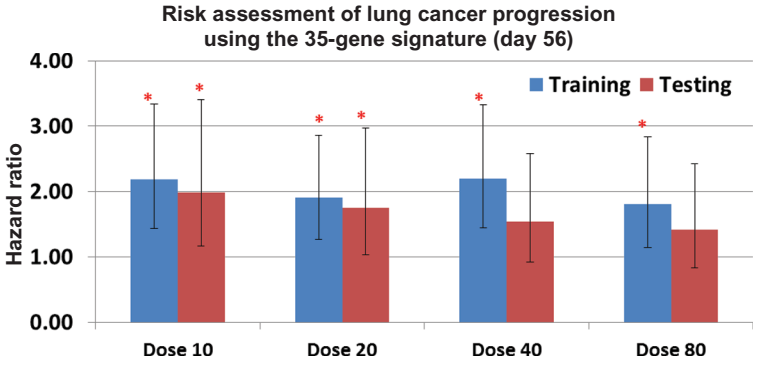

FIGURE 3. Hazard ratio in risk assessment of lung cancer progression for each dose at d 56 using the 35-gene signature in the training cohort (UM and HLM) and testing cohort (MSK and DFCI). The expression centroid in each group of mice ($n = 8$) treated with different doses of MWCNT were used to predict the risk of lung cancer progression and metastasis in both training and test sets, respectively. The cutoff value that generated significant hazard ratio in the training set was validated in the test set. The asterisk above the error bar indicates the hazard ratio of death from lung cancer is statistically significant ($p < .05$) (color figure available online).

TABLE 5. Risk Prediction of Lung Cancer Initiation on Spira et al. (2007) With the 35-Gene Signature

	Sensitivity (lung cancer)	Specificity (normal)	Accuracy	Odds ratio [95% CI]	*p* Value
Training ($n = 77$)	68% (27/40)	57% (21/37)	62%	2.73 [1.08, 6.89]	.03
Test 1 ($n = 52$)	80% (16/20)	63% (20/32)	69%	6.67 [1.80, 24.68]	.004
Test 2 ($n = 35$)	94% (17/18)	65% (11/17)	80%	31.16 [3.29, 295.04]	.002

TABLE 6. Risk Prediction of Lung Cancer Initiation on Spira et al. (2007) With the 16-Gene Signature

	Sensitivity (lung cancer)	Specificity (normal)	Accuracy	Odds ratio [95% CI]	*p* Value
Training ($n = 77$)	75% (30/40)	57% (21/37)	66%	3.94 [1.50, 10.36]	.005
Test 1 ($n = 52$)	85% (17/20)	75% (24/32)	79%	17 [3.93, 73.57]	.0002
Test 2 ($n = 35$)	72% (13/18)	71% (12/17)	71%	6.24 [1.44, 27.06]	.014

to classify lung cancer patients from normal individuals in the training set, respectively. Each gene signature was then evaluated with two test sets, without re-estimating the model parameters.

Using a Random committee algorithm, the 35-gene signature classified lung cancer patients from normal patients with an overall accuracy of 69% in Test set 1 and 80% in Test set 2 (Table 5). The sensitivity in predicting lung cancer is 80% in Test set 1 and 94% in Test set 2. The specificity in correctly classified normal individuals is 63% in Test set 1, and 65% in Test set 2. The OR of predicted lung cancer risk was significant in both test sets ($OR = 6.67$, 95% CI: [1.80, 24.68] in Test set 1; $OR = 31.16$, 95% CI: [3.29, 295.04] in Test set 2; Table 5).

Using a JRip algorithm, the 16-gene signature predicted lung cancer risk with an overall accuracy of 79% in Test set 1 and 71% in Test set 2 (Table 6). The sensitivity in predicting lung cancer is 85% in Test set 1 and 72% in Test set 2. The specificity in correctly classified normal individuals is 75% in Test set 1 and 71% in Test set 2. The OR of predicted lung cancer risk was statistically significant in both test sets ($OR = 17$, 95% CI: [3.93, 73.57] in Test set 1; $OR = 6.24$, 95% CI: [1.44, 27.06] in Test set 2; Table 6). These results suggested an association between MWCNT-induced gene signatures and human lung cancer risk.

To investigate whether these two gene signatures were concordant in predicting human lung cancer risk, chi-squared analysis was carried out to test the association between these two risk assessment models. Due to the small sample size, the two independent test sets from Spira et al. (2007) were combined in the analysis. The results demonstrate that the two gene signatures were strongly associated ($P < 7.41E\text{-}16$) on predictions of human lung cancer risk (Table 7). These results indicate that these two gene signatures might cover a largely concordant genomic space of lung cancer, although there are only three overlapping genes (IL6, MSR1, and SPP1) between them.

TABLE 7. Chi-Squared Test on the Lung Cancer Risk Prediction of the Two Signatures on Combined Test Sets on Spira et al. (2007)

	Prediction by the 35-gene signature		
	Cancer	Normal	Test statistics
Prediction by the 16-gene signature			
Cancer	36	7	$\chi^2 = 20.08$
Normal	15	29	$P = 7.41E\text{-}6$

DISCUSSION

MWCNT are man-made fiber-shaped materials. Their potential fiber toxicity is mainly due to their high aspect ratio and micrometer length (Stanton et al. 1981). An asbestos-like acute inflammatory effect

was observed upon the administration of long MWCNT into abdominal cavity of mice (Poland et al. 2008). It was found that long fibers of MWCNT induced inflammation and granulomas at the peritoneal side of the diaphragm at 24 h and 7 d postexposure, while short fibers of MWCNT failed to induce abdominal inflammation or granulomas, indicating MWCNT-induced asbestos-like effects were fiber length dependent. A study found that intra-abdominal exposure to MWCNT induced mesothelioma, a form of cancer in body cavity linings, after a year postexposure in $p53^{+/-}$ mice (Takagi et al. 2008). In this study, several asbestos-like pathological changes, such as fibrous scars, granulomas, and typical mesotheliomas, were found in the peritoneal cavity of MWCNT-treated $p53^{+/-}$ mice by histopathological analysis (Takagi et al. 2008). The characteristic histopathological changes of MWCNT-induced mesotheliomas were hobnail appearance to large tumors along with high mitotic rate cells and central necrosis due to a high grade of malignant mesothelioma, indicating that characteristic carcinogenic mechanisms were involved (Takagi et al. 2008). Recently, several studies demonstrated that MWCNT reached the pleural tissue in mice, the site of mesothelioma, after pulmonary exposure to occupationally relevant burdens of MWCNT (Mercer et al. 2010; Ryman-Rasmussen et al. 2009). Taken together, these studies suggest that fibrous structure of MWCNT may pose a carcinogenic risk on humans similar to that of asbestos fibers.

Several studies found that MWCNT were persistent in lungs up to 60 d postexposure (Muller et al. 2005; Porter et al. 2010), and histopathological analysis demonstrated that upon pulmonary exposure to MWCNT the particles penetrated through alveolar walls and were transported to the alveolar interstitium, subpleural tissue, and subpleural lymphatics, finally reaching the intrapleural space (Mercer et al. 2011; Porter et al. 2010). These results show that MWCNT exposure has a pattern of biopersistence and pulmonary penetration similar to that of asbestos (Elgrabli et al. 2008; Kim et al. 2010), which may be associated with the potential MWCNT-induced pathogenicity and carcinogenesis. It has been well established that the biopersistence and pulmonary penetration potential of asbestos are critical factors involved in asbestos-induced pathogenicity and carcinogenesis (Shukla et al. 2003; Vallyathan et al. 1998). Taken together, the genotoxicity of MWCNT, their fibrous characteristics, and their biopersistence and pulmonary penetration potential have promoted the hypothesis that exposure to MWCNT may contribute to the initiation and the progression of asbestos-like pathological responses, such as lung carcinogenesis (Donaldson et al. 2006; Pacurari et al. 2010).

Previously, a study was conducted to investigate how MWCNT exposure affected the lung cancer prognostic biomarkers and the related cancer signaling pathways in mouse lungs (Pacurari et al. 2011). In total, 63 identified lung cancer prognostic biomarker genes and major signaling biomarker genes (Guo et al. 2006 2008; Wan et al. 2010) were analyzed in mouse lungs exposed to 0, 10 20, 40, or 80 μg of MWCNT by pharyngeal aspiration at 7 and 56 d postexposure using quantitative PCR assays. At 7 and 56 d postexposure, a set of 7 genes and a set of 11 genes, respectively, showed differential expression in the lungs of mice exposed to MWCNT versus the control group. Ingenuity Pathway Analysis (IPA) found that several carcinogenic-related signaling pathways and carcinogenesis itself were associated with both the 7- and 11-gene signatures. The results demonstrated that MWCNT exposure induces changes in lung cancer biomarker gene expression in mouse lungs, which may indicate a potential association between MWCNT exposure-induced lung inflammatory damage and fibrotic responses and lung carcinogenesis. The results of the IPA also indicated that MWCNT exposure may induce alterations in several fibrosis and cancer-related signaling transduction pathways (Pacurari et al. 2011).

Based on the results from the previous cancer-focused gene expression analyses in MWCNT-exposed mouse lungs (Pacurari et al. 2011), the present study sought to identify MWCNT-induced gene expression signatures

from the entire genome. Further, this study attempted to explore whether these gene signatures correlated with human lung cancer risk and progression in a group of cancer patients. The design of this study was established based on our previous in vivo mouse model for pharyngeal aspiration of MWCNT (Porter et al. 2010). The mouse lung tissue specimens at 1, 7, 28, and 56 d post MWCNT exposure were taken from the previous investigation for the genome-wide expression studies. The 35-gene signature derived from the "56-day cancer related gene set" was found to predict the risk of cancer progression and metastasis in human lung adenocarcinoma patients. In this analysis, the expression profiles in MWCNT-treated mice could be used to identify more aggressive tumors from the tumors with the same disease stage (stage 1 tumors). Specifically, the gene expression profiles in the mice treated with dose 10 and 20 μg may categorize lung adenocarcinoma tumors into metastatic and nonmetastatic groups with distinct disease-specific survival in both training and testing patient cohorts. Lung adenocarcinoma patients having a gene expression pattern more similar to that in the MWCNT-treated mice had more aggressive tumors with a poor clinical outcome; whereas patient tumors showing a less similar gene expression pattern to that in the MWCNT-treated mice had less metastatic potential with a relatively better clinical outcome. The specificity of the cancer progression predictions was above 86% in both training and testing patient cohorts, indicating that the 35-gene signature in MWCNT-treated mice might predict the metastatic potential in human lung adenocarcinoma patients. The identified gene signature is unique and is different from previous published gene signatures for breast cancer (Perou et al. 2000; Sorlie et al. 2003; Sotiriou et al. 2003; van 't Veer et al. 2002), colon cancer (Barrier et al. 2005 2006 2007), and leukemia (Langer et al. 2008; Payton et al. 2009). It is also different from breast cancer gene signatures (Habermann et al. 2009; Ma et al. 2007) previously identified by our group.

This study used the nearest centroid classification method to predict human lung cancer progression by measuring the correlation between mouse gene expression data and patient gene expression profiles. This algorithm is robust to account for different microarray platforms, in this case, even the different species. This algorithm was successfully used to classify breast cancer subtypes in clinics based on gene expression profiles quantified with different microarray platforms (Perou et al. 1999; 2000; Sorlie et al. 2003).

Both MWCNT and asbestos induce pulmonary fibrosis. However, asbestos-induced fibrosis is associated with persistent pulmonary inflammation and damage (Goodglick and Kane 1990; Pacurari et al. 2010), whereas MWCNT-induced fibrosis is not associated with persistent pulmonary inflammation and damage (Porter et al. 2010). It was found that upon MWCNT exposure, pulmonary inflammation and damage peaked at 1–7 d post-exposure while pulmonary fibrosis progresses through 28–56 d postexposure (Mercer et al. 2011; Porter et al. 2010). These results indicate that the molecular events that lead to fibrosis induced by asbestos and MWCNT may be different. Indeed, recent in vitro studies demonstrated that carbon nanotubes directly stimulate collagen production of lung fibroblasts and fibroblast proliferation (Wang et al. 2010a; 2010b). Therefore, MWCNT-induced fibrosis may result from the laying down of a matrix that induces fibroblast growth and activation. In terms of genotoxic effects of MWCNT and asbestos, it was demonstrated that MWCNT interact with cellular biomolecules, such as the centrosomes and mitotic spindles, as well as the motor proteins that separate the chromosomes during cell division, leading to monopolar divisions of chromosomes. The resulting aneuploidy was proposed as a major molecular mechanism involved in potential MWCNT-induced carcinogenesis (Sargent et al. 2010). In contrast, reactive oxygen species (ROS)-induced DNA damage is a key molecular mechanism involved in asbestos-induced carcinogenesis. Since mechanisms of action between MWCNT and asbestos may differ and asbestos exposure may induce different gene signature in mouse lungs, the use of asbestos as a positive control in this study and comparison to MWCNT-induced gene signatures may not

be of unique value. For this reason, gene induction following asbestos exposure to mouse lungs was not evaluated in the current study.

In the current study, tangled CNT (agglomerated form) was not selected as a negative control because the distinction between dispersed MWCNT and tangled CNT is not an all-or-none situation. A study has shown that tangled CNT can disperse in the mouse lungs over time (Shvedova et al. 2012). Therefore, tangled CNT may not be an ideal negative control for our 56-d postexposure evaluation study.

NIOSH scientists have reviewed the literatures currently available concerning the pulmonary effects of exposure to SWCNT, MWCNT, and carbon nanofibers (Castranova et al. 2012; NIOSH 2011). In general, these carbon-based fibrous nanoparticles each produced a rapid but transient pulmonary inflammation and injury, granulomatous lesions at deposition sites of agglomerated structures, and rapid and progressive alveolar interstitial fibrosis associated with deposition of more dispersed structures. Although quantitative responses among studies using different types of CNT demonstrated some differences in potency, qualitatively, the responses were similar. Therefore, gene signatures identified in this study may well be generalizable to CNT as a class of fibrous nanoparticles.

It is noteworthy that several genes in the 35-gene MWCNT signature encode proteins that are involved in lung cancer development and progression. Cysteine protease cathepsin B (CTSB) plays an important role in lung cancer progression and metastasis (Vasiljeva et al. 2006). Epidermal growth factor receptor (EGFR) is essential in lung carcinogenesis through modulating cell proliferation, apoptosis, cell motility, and neovascularization (Cheng et al. 2012). Insulin-like growth factor 1 (IGF1) is a key mediator of growth hormone-related signaling transduction and plays a key role in the pathogenesis of lung cancer (Furstenberger and Senn 2002). IKBKG (inhibitor of nuclear factor kappa-B kinase subunit gamma) is the regulatory subunit of the inhibitor of IKB kinase, which is essential for the survival of non-small-cell lung cancer (Shen and Hahn 2011). Interlukin-6 (IL-6) is a proinflammatory cytokine that is associated with lung cancer progression through the inhibition of apoptosis and the stimulation of angiogenesis (Lukaszewicz et al. 2007). Matrix metalloproteinases (MMP) are members of the metzincin group of proteases, and regulate extracellular tissue signaling networks. Disruption of the MMP activities plays a key role in the development of pulmonary diseases, including lung cancer (Vandenbroucke et al. 2011). SOX9 is a major transcription factor required for lung cancer development (Jiang et al. 2010). SPP1 (osteopontin) is one of the most abundantly expressed proteins and plays a regulatory role in a range of lung diseases, including pulmonary granuloma formation, fibrosis, and malignancy (O'Regan 2003). It was also found that the changes in gene expression levels of two genes, GSK3B and MSK1, in the 35-gene signature are associated with lung cancer progression and outcome (Chari et al. 2007; Ohtaki et al. 2010). DNA methylation changes of two genes, EYA 4 and DAPK1, are associated with lung cancer development (Scesnaite et al. 2012; Selamat et al. 2011). Moreover, CDKN3, IL1A, and PBK have been identified as prediction biomarkers of lung cancer development and prognosis (MacDermed et al. 2010; Shih et al. 2011; Van Dyke et al. 2009).

In the present study, the lung tissue specimens were collected from the mice exposed to MWCNT from 1 to 56 d postexposure, which was not sufficient for mice to develop lung cancer. Vaslet et al. (2002) demonstrated that asbestos exposure induces malignant mesothelioma in mouse lungs at 60 wk postexposure. In humans, the latency period between the first exposure to asbestos and diagnosis of mesothelioma ranges from 20 to 40 yr (Pacurari et al. 2010). Therefore, MWCNT would not be expected to induce lung carcinogenesis at 56 d postexposure. However, in vivo animal model-generated gene profiling would reveal the information that approximates the complexity of the human body and its cellular, biochemical, and molecular systems that are involved in responses to chemical agents. The

unique advantage of the present study is the ability to detect responses at the molecular level that may lead to pathology long before the clinical symptoms occur. The emphasis of this study is on the predication of potential risk or toxicity at the early stage. The ability of MWCNT-induced gene sets to correlate with carcinogenesis of lung cancer patients provides justification for a further long-term study to determine the temporal association between MWCNT-induced gene alterations and development of precancerous lesions and/or tumors in the mouse lung. Such a study was proposed, peer-reviewed, and currently underway in our laboratory.

Several studies showed that animal model-based gene expression profiling can successfully predict human target organ toxicities for numerous human diseases, including cancer (Newton et al. 2004; Nuwaysir et al. 1999). Using gene expression profiling to predict chemical toxicity was proposed and applied in genotoxicity for several decades (Aubrecht and Caba 2005). The newly developed high-throughput-based global gene expression profiling techniques have made it possible to identify key predictive gene signatures from various specimens. It has become increasingly important to use gene expression signatures identified with bioinformatics methods for toxicity predication (Shi et al. 2010), risk assessment, and screening (Afshari et al. 2011). In the case of asbestos exposure, a gene expression and copy number profiling study was conducted to identify important allelic imbalance in asbestos-related lung cancer (Wikman et al. 2007). Gene expression signatures identified from blood specimens in APAP-exposed rats have been used to predict exposure levels of APAP in humans (Bushel et al. 2007).

Similarly, the present study sought to identify MWCNT-induced gene signatures in an animal model that may potentially be useful for the prediction of lung cancer initiation and/or progression, well before the tumor is detected by morphological assessments. The relatively short duration of present study does not allow one to address whether MWCNT would induce lung tumors. However, our data indicate a correlation between MWCNT-induced gene expression changes in the mouse lung and similar gene expression changes associated with human lung cancer risk and progression. Such an approach has been used for biomarker-based risk assessment of APAP (Bushel et al. 2007). Given the nature of biomarker research, clinically applied biomarkers need to be validated in the following three phases: retrospective studies, prospective evaluation, and clinical trials. The current study that utilized multiple retrospective patient cohorts to validate the identified biomarker genes is an initial step, that is, the identification of potentially useful gene signatures for further study. In order to develop a clinically applicable gene test for medical surveillance, the following studies need to be carried out: (1) a chronic animal study to determine the temporal relationship between gene alterations and formation of precancer lesions and/or tumors; (2) the comparison of such gene signatures with those associated with human lung cancers; (3) development of a noninvasive blood test; and (4) prospective longitudinal evaluation of the identified gene test in animal models and human subjects. A project was initiated within NIOSH to evaluate lung tumor formation over the course of 1 yr after a 2-wk inhalation of MWCNT in a cancer-susceptible mouse strain. The time course of gene changes in lung tissue will be determined and the blood samples will be used to assess the predictive power of the identified biomarkers. Hopefully, the present study is the first step in the development of a surveillance approach for early detection of lung cancer and prognosis with MWCNT in the workplace.

Gene expression profiling has yielded two commercially available, clinically used breast cancer prognostic tests, MammaPrint (van 't Veer et al. 2002; van de Vijver et al. 2002) and Oncotype DX (Paik et al. 2004). In these routine clinical gene tests, mRNA expression, not protein expression, is used to predict clinical outcome in patients. The commonly accepted approach in these biomarker studies is to use mRNA expression for clinical diagnosis or prognosis, instead of protein expression. This is

because mRNA quantification is considered reliable for clinical tests, whereas current protein expression assays, such as immunohistochemistry or Western blots, are semiquantitative and thus are not favored for developing multiple-gene assays as clinical tests.

A recent study showed that chronic exposure to carbon nanotubes produced malignant transformation of human lung epithelial cells, which in turn induce tumorigenesis in xenograft mice (Wang et al. 2011). Mounting evidence has indicated potential health hazards, including carcinogenesis implications, associated with carbon nanotube exposures. In order to develop reliably assays for risk assessment of potential lung cancer tumorigenesis and progression, the present study undertook a genome-scale expression approach using an in vivo mouse model. The study results demonstrate that MWCNT exposure induces selective gene expression changes in an analysis of the entire genome. In particular, the identified 56-d gene signature in mice contained cancer-related genes and may accurately predict human lung adenocarcinoma progression and prognosis, with high specificity in a patient cohort. This gene signature of response in the mouse model to MWCNT was found useful in assessing the risk for human lung cancer recurrence and metastasis. Furthermore, this 35-gene signature and a set of 16 genes consistently changing at multiple postexposure time intervals and treatment doses of MWCNT with significant linear dose response in the time course might also predict human lung cancer risk. The microarray results have been validated with quantitative reverse-transcription polymerase chain reaction (RT-PCR) analyses in a separate study (Pacurari et al. 2011). The selection of 16 genes that were changed at two time points was aimed to identify genes that were consistently changed by MWCNT, and these gene expression changes were not transient or reversible over the time course up to 56 d postexposure. It is likely that this set of genes is also associated with other diseases, in addition to lung cancer risk.

This article focused on the identification of gene signatures with potential applications on risk assessment of MWCNT-induced lung cancer risk and progression. Our genome-wide expression studies show that the MWCNT-induced gene alterations (in more than 3000 significant genes) have implications on multiple diseases and disorders, including inflammation, fibrosis, and cardiovascular disease, among many others (which will be discussed in a separate article). In order to facilitate the analysis of specific gene expression changes and biological processes (such as oxidative stress) in response to MWCNT exposure, a website (http://www.mwcnttranscriptome.org) was developed to query MWCNT-induced gene expression. Although the current animal study did not observe tumor formation in response to MWCNT exposure and the analyzed human samples were not previously exposed to MWCNT, the similarity between the genomic characteristics induced by MWCNT exposure in mice and those associated with human lung cancer initiation and progression suggests a significant association between MWCNT-induced gene alterations and clinical phenotypes in human lung cancer patients. In conclusion, the identified MWCNT-induced gene expression signatures may be useful for risk assessments and medical surveillance, with clinical implications in early detection of lung cancer and prognosis. To provide further support for this application, a 1-yr evaluation after a 2-wk inhalation of MWCNT is currently being conducted in our laboratory to correlate time-dependent alterations in gene expression with development of precancerous lesions and/or tumor formation.

REFERENCES

Afshari, C. A., Hamadeh, H. K., and Bushel, P. R. 2011. The evolution of bioinformatics in toxicology: advancing toxicogenomics. *Toxicol. Sci.* 120(suppl. 1): S225–37.

Amin, R. P., Vickers, A. E., Sistare, F., Thompson, K. L., Roman, R. J., Lawton, M., Kramer, J., Hamadeh, H. K., Collins, J., Grissom, S., Bennett, L., Tucker, C. J., Wild, S.,

Kind, C., Oreffo, V., Davis, J. W. 2nd, Curtiss, S., Naciff, J. M., Cunningham, M., Tennant, R., Stevens, J., Car, B., Bertram, T. A., and Afshari, C. A. 2004. Identification of putative gene based markers of renal toxicity. *Environ. Health Perspect*. 112: 465–79.

Aschberger, K., Johnston, H. J., Stone, V., Aitken, R. J., Hankin, S. M., Peters, S. A., Tran, C. L., and Christensen, F. M. 2010. Review of carbon nanotubes toxicity and exposure—Appraisal of human health risk assessment based on open literature. *Crit. Rev. Toxicol*. 40: 759–90.

Aubrecht, J., and Caba, E. 2005. Gene expression profile analysis: an emerging approach to investigate mechanisms of genotoxicity. *Pharmacogenomics* 6: 419–28.

Auerbach, O., Garfinkel, L., and Parks, V. R. 1979. Scar cancer of the lung: Increase over a 21 year period. *Cancer* 43: 636–42.

Barrier, A., Boelle, P. Y., Roser, F., Gregg, J., Tse, C., Brault, D., Lacaine, F., Houry, S., Huguier, M., Franc, B., Flahault, A., Lemoine, A., and Dudoit, S. 2006. Stage II colon cancer prognosis prediction by tumor gene expression profiling. *J. Clin. Oncol*. 24: 4685–91.

Barrier, A., Lemoine, A., Boelle, P. Y., Tse, C., Brault, D., Chiappini, F., Breittschneider, J., Lacaine, F., Houry, S., Huguier, M., Van der Laan, M. J., Speed, T., Debuire, B., Flahault, A., and Dudoit, S. 2005. Colon cancer prognosis prediction by gene expression profiling. *Oncogene* 24: 6155–64.

Barrier, A., Roser, F., Boelle, P. Y., Franc, B., Tse, C., Brault, D., Lacaine, F., Houry, S., Callard, P., Penna, C., Debuire, B., Flahault, A., Dudoit, S., and Lemoine, A. 2007. Prognosis of stage II colon cancer by non-neoplastic mucosa gene expression profiling. *Oncogene* 26: 2642–48.

Bushel, P. R., Heinloth, A. N., Li, J., Huang, L., Chou, J. W., Boorman, G. A., Malarkey, D. E., Houle, C. D., Ward, S. M., Wilson, R. E., Fannin, R. D., Russo, M. W., Watkins, P. B., Tennant, R. W., and Paules, R. S. 2007. Blood gene expression signatures predict exposure levels. *Proc. Natl. Acad. Sci. USA* 104: 18211–16.

Castranova, V., Schulte, P. A., and Zumwalde, R. D. 2012. Occupational nanosafety considerations for carbon nanotubes and carbon nanofibers. *Accounts Chem. Res.*, in press.

Chari, R., Lonergan, K. M., Ng, R. T., MacAulay, C., Lam, W. L., and Lam, S. 2007. Effect of active smoking on the human bronchial epithelium transcriptome. *BMC Genomics* 8: 297.

Cohen, W.W. 1995. Fast effective rule induction. *Proc. Twelfth Int. Conf. Machine Learning*, 115–23.

Cheng, L., Alexander, R. E., Maclennan, G. T., Cummings, O. W., Montironi, R., Lopez-Beltran, A., Cramer, H. M., Davidson, D. D., and Zhang, S. 2012. Molecular pathology of lung cancer: Key to personalized medicine. *Mod. Pathol.*, in press.

Director's Challenge Consortium for the Molecular Classification of Lung, Shedden, K., Taylor, J. M., Enkemann, S. A., Tsao, M. S., Yeatman, T. J., Gerald, W. L., Eschrich, S., Jurisica, I., Giordano, T. J., Misek, D. E., Chang, A. C., Zhu, C. Q., Strumpf, D., Hanash, S., Shepherd, F. A., Ding, K., Seymour, L., Naoki, K., Pennell, N., Weir, B., Verhaak, R., Ladd-Acosta, C., Golub, T., Gruidl, M., Sharma, A., Szoke, J., Zakowski, M., Rusch, V., Kris, M., Viale, A., Motoi, N., Travis, W., Conley, B., Seshan, V. E., Meyerson, M., Kuick, R., Dobbin, K. K., Lively, T., Jacobson, J. W., and Beer, D. G. 2008. Gene expression-based survival prediction in lung adenocarcinoma: A multisite, blinded validation study. *Nat. Med*. 14: 822–27.

Donaldson, K., Aitken, R., Tran, L., Stone, V., Duffin, R., Forrest, G., and Alexander, A. 2006. Carbon nanotubes: A review of their properties in relation to pulmonary toxicology and workplace safety. *Toxicol. Sci*. 92: 5–22.

Elgrabli, D., Floriani, M., Abella-Gallart, S., Meunier, L., Gamez, C., Delalain, P., Rogerieux, F., Boczkowski, J., and Lacroix, G. 2008. Biodistribution and clearance of instilled carbon nanotubes in rat lung. *Part. Fibre Toxicol*. 5: 20.

Elick, C. F., Rouhana, A., and Bagherjeiran, A. 2006. Using clustering to learn distance functions for supervised similarity assessment. *Eng. Appl. Artif. Intelligence* 19: 395–401.

Elliott, R. L., and Blobe, G. C. 2005. Role of transforming growth factor Beta in human cancer. *J. Clin. Oncol.* 23: 2078–93.

Furstenberger, G., and Senn, H. J. 2002. Insulin-like growth factors and cancer. *Lancet Oncol.* 3: 298–302.

Goodglick, L. A., and Kane, A. B. 1990. Cytotoxicity of long and short crocidolite asbestos fibers in vitro and in vivo. *Cancer Res.* 50: 5153–63.

Guo, L., Ma, Y., Ward, R., Castranova, V., Shi, X., and Qian, Y. 2006. Constructing molecular classifiers for the accurate prognosis of lung adenocarcinoma. *Clin. Cancer Res.* 12: 3344–54.

Guo, N. L., Wan, Y. W., Tosun, K., Lin, H., Msiska, Z., Flynn, D. C., Remick, S. C., Vallyathan, V., Dowlati, A., Shi, X., Castranova, V., Beer, D. G., and Qian, Y. 2008. Confirmation of gene expression-based prediction of survival in non-small cell lung cancer. *Clin. Cancer Res.* 14: 8213–20.

Habermann, J. K., Doering, J., Hautaniemi, S., Roblick, U. J., Bundgen, N. K., Nicorici, D., Kronenwett, U., Rathnagiriswaran, S., Mettu, R. K., Ma, Y., Kruger, S., Bruch, H. P., Auer, G., Guo, N. L., and Ried, T. 2009. The gene expression signature of genomic instability in breast cancer is an independent predictor of clinical outcome. *Int. J. Cancer* 124: 1552–64.

Hamadeh, H. K., Jayadev, S., Gaillard, E. T., Huang, Q., Stoll, R., Blanchard, K., Chou, J., Tucker, C. J., Collins, J., Maronpot, R., Bushel, P., and Afshari, C. A. 2004. Integration of clinical and gene expression endpoints to explore furan-mediated hepatotoxicity. *Mutat. Res.* 549: 169–83.

Hamadeh, H. K., Knight, B. L., Haugen, A. C., Sieber, S., Amin, R. P., Bushel, P. R., Stoll, R., Blanchard, K., Jayadev, S., Tennant, R. W., Cunningham, M. L., Afshari, C. A., and Paules, R. S. 2002. Methapyrilene toxicity: Anchorage of pathologic observations to gene expression alterations. *Toxicol. Pathol.* 30: 470–82.

Jagirdar, J., Lee, T. C., Reibman, J., Gold, L. I., Aston, C., Begin, R., and Rom, W. N. 1997. Immunohistochemical localization of transforming growth factor beta isoforms in asbestos-related diseases. *Environ. Health Perspect.* 105(suppl. 5):1197–203.

Jiang, S. S., Fang, W. T., Hou, Y. H., Huang, S. F., Yen, B. L., Chang, J. L., Li, S. M., Liu, H. P., Liu, Y. L., Huang, C. T., Li, Y. W., Jang, T. H., Chan, S. H., Yang, S. J., Hsiung, C. A., Wu, C. W., Wang, L. H., and Chang, I. S. 2010. Upregulation of SOX9 in lung adenocarcinoma and its involvement in the regulation of cell growth and tumorigenicity. *Clin. Cancer Res.* 16: 4363–73.

Karlsson, H. L., Cronholm, P., Gustafsson, J., and Moller, L. 2008. Copper oxide nanoparticles are highly toxic: A comparison between metal oxide nanoparticles and carbon nanotubes. *Chem Res Toxicol* 21: 1726–32.

Kim, J. E., Lim, H. T., Minai-Tehrani, A., Kwon, J. T., Shin, J. Y., Woo, C. G., Choi, M., Baek, J., Jeong, D. H., Ha, Y. C., Chae, C. H., Song, K. S., Ahn, K. H., Lee, J. H., Sung, H. J., Yu, I. J., Beck, G. R., Jr., and Cho, M. H. 2010. Toxicity and clearance of intratracheally administered multiwalled carbon nanotubes from murine lung. *J. Toxicol. Environ. Health A* 73: 1530–43.

Kobayashi, N., Naya, M., Ema, M., Endoh, S., Maru, J., Mizuno, K., and Nakanishi, J. 2010. Biological response and morphological assessment of individually dispersed multi-wall carbon nanotubes in the lung after intratracheal instillation in rats. *Toxicology* 276: 143–53.

Lam, C. W., James, J. T., McCluskey, R., and Hunter, R. L. 2004. Pulmonary toxicity of single-wall carbon nanotubes in mice 7 and 90 days after intratracheal instillation. *Toxicol. Sci.* 77: 126–34.

Langer, C., Radmacher, M. D., Ruppert, A. S., Whitman, S. P., Paschka, P., Mrozek, K., Baldus, C. D., Vukosavljevic, T., Liu, C. G., Ross, M. E., Powell, B. L., de la Chapelle, A., Kolitz, J. E., Larson, R. A., Marcucci, G., Bloomfield, C. D., Cancer and Leukemia

Group B. 2008. High BAALC expression associates with other molecular prognostic markers, poor outcome, and a distinct gene-expression signature in cytogenetically normal patients younger than 60 years with acute myeloid leukemia: A Cancer and Leukemia Group B (CALGB) study. *Blood* 111: 5371–79.

Levner, I. 2005. Feature selection and nearest centroid classification for protein mass spectrometry. *BMC Bioinformatics* 6: 68.

Luhe, A., Hildebrand, H., Bach, U., Dingermann, T., and Ahr, H. J. 2003. A new approach to studying ochratoxin A (OTA)-induced nephrotoxicity: Expression profiling in vivo and in vitro employing cDNA microarrays. *Toxicol. Sci.* 73: 315–28.

Lukaszewicz, M., Mroczko, B., and Szmitkowski, M. 2007. [Clinical significance of interleukin-6 (IL-6) as a prognostic factor of cancer disease]. *Pol. Arch. Med. Wewn.* 117: 247–51.

Ma, Y., Qian, Y., Wei, L., Abraham, J., Shi, X., Castranova, V., Harner, E. J., Flynn, D. C., and Guo, L. 2007. Population-based molecular prognosis of breast cancer by transcriptional profiling. *Clin. Cancer Res.* 13: 2014–22.

MacDermed, D. M., Khodarev, N. N., Pitroda, S. P., Edwards, D. C., Pelizzari, C. A., Huang, L., Kufe, D. W., and Weichselbaum, R. R. 2010. MUC1-associated proliferation signature predicts outcomes in lung adenocarcinoma patients. *BMC Med. Genomics* 3: 16.

MacKinnon, A.C., Kopatz, J., and Sethi, T. 2010. The molecular and cellular biology of lung cancer: identifying novel therapeutic strategies. *Br Med Bull* 95: 47–61.

Mercer, R. R., Hubbs, A. F., Scabilloni, J. F., Wang, L., Battelli, L. A., Friend, S., Castranova, V., and Porter, D. W. 2011. Pulmonary fibrotic response to aspiration of multi-walled carbon nanotubes. *Part Fibre Toxicol* 8: 21.

Mercer, R. R., Hubbs, A. F., Scabilloni, J. F., Wang, L., Battelli, L. A., Schwegler-Berry, D., Castranova, V., and Porter, D. W. 2010. Distribution and persistence of pleural penetrations by multi-walled carbon nanotubes. *Part. Fibre Toxicol.* 7: 28.

Muller, J., Decordier, I., Hoet, P. H., Lombaert, N., Thomassen, L., Huaux, F., Lison, D., and Kirsch-Volders, M. 2008. Clastogenic and aneugenic effects of multi-wall carbon nanotubes in epithelial cells. *Carcinogenesis* 29: 427–33.

Muller, J., Huaux, F., Moreau, N., Misson, P., Heilier, J. F., Delos, M., Arras, M., Fonseca, A., Nagy, J. B., and Lison, D. 2005. Respiratory toxicity of multi-wall carbon nanotubes. *Toxicol. Appl. Pharmacol.* 207: 221–31.

Nagai, H., Okazaki, Y., Chew, S. H., Misawa, N., Yamashita, Y., Akatsuka, S., Ishihara, T., Yamashita, K., Yoshikawa, Y., Yasui, H., Jiang, L., Ohara, H., Takahashi, T., Ichihara, G., Kostarelos, K., Miyata, Y., Shinohara, H., and Toyokuni, S. 2011. Diameter and rigidity of multiwalled carbon nanotubes are critical factors in mesothelial injury and carcinogenesis. *Proc. Natl. Acad. Sci. USA* 108: E1330–E1338.

Newton, R. K., Aardema, M., and Aubrecht, J. 2004. The utility of DNA microarrays for characterizing genotoxicity. *Environ. Health Perspect.* 112: 420–422.

National Institute for Occupational Safety and Health. 2011. Current intelligence bulletin: Occupational exposure to carbon nanotubes and nanofibers. www.cdc.gov/niosh/docket/review/docket 161A

Nuwaysir, E. F., Bittner, M., Trent, J., Barrett, J. C., and Afshari, C. A. 1999. Microarrays and toxicology: the advent of toxicogenomics. *Mol. Carcinogen.* 24:153–159.

O'Regan, A. 2003. The role of osteopontin in lung disease. *Cytokine Growth Factor Rev.* 14: 479–88.

Ohtaki, Y., Ishii, G., Nagai, K., Ashimine, S., Kuwata, T., Hishida, T., Nishimura, M., Yoshida, J., Takeyoshi, I., and Ochiai, A. 2010. Stromal macrophage expressing CD204 is associated with tumor aggressiveness in lung adenocarcinoma. *J. Thorac. Oncol.* 5: 1507–15.

Pacurari, M., Castranova, V., and Vallyathan, V. 2010. Single- and multi-wall carbon nanotubes versus asbestos: Are the carbon nanotubes a new health risk to humans? *J. Toxicol. Environ. Health A* 73: 378–95.

Pacurari, M., Qian, Y., Porter, D. W., Wolfarth, M., Wan, Y., Luo, D., Ding, M., Castranova, V., and Guo, N. L. 2011. Multi-walled carbon nanotube-induced gene expression in the mouse lung: Association with lung pathology. *Toxicol. Appl. Pharmacol.* 255: 18–31.

Paik, S., Shak, S., Tang, G., Kim, C., Baker, J., Cronin, M., Baehner, F. L., Walker, M. G., Watson, D., Park, T., Hiller, W., Fisher, E. R., Wickerham, D. L., Bryant, J., and Wolmark, N. 2004. A multigene assay to predict recurrence of tamoxifen-treated, node-negative breast cancer. *N. Engl. J. Med.* 351: 2817–26.

Paules, R. 2003. Phenotypic anchoring: Linking cause and effect. *Environ. Health Perspect.* 111: A338–39.

Payton, J. E., Grieselhuber, N. R., Chang, L. W., Murakami, M., Geiss, G. K., Link, D. C., Nagarajan, R., Watson, M. A., and Ley, T. J. 2009. High throughput digital quantification of mRNA abundance in primary human acute myeloid leukemia samples. *J. Clin. Invest.* 119: 1714–26.

Peretz, A., Checkoway, H., Kaufman, J. D., Trajber, I., and Lerman, Y. 2006. Silica, silicosis, and lung cancer. *Isr. Med. Assoc. J.* 8: 114–18.

Perou, C. M., Jeffrey, S. S., van de Rijn, M., Rees, C. A., Eisen, M. B., Ross, D. T., Pergamenschikov, A., Williams, C. F., Zhu, S. X., Lee, J. C., Lashkari, D., Shalon, D., Brown, P. O., and Botstein, D. 1999. Distinctive gene expression patterns in human mammary epithelial cells and breast cancers. *Proc. Natl. Acad. Sci. USA* 96: 9212–17.

Perou, C. M., Sorlie, T., Eisen, M. B., van de Rijn, M., Jeffrey, S. S., Rees, C. A., Pollack, J. R., Ross, D. T., Johnsen, H., Akslen, L. A., Fluge, O., Pergamenschikov, A., Williams, C., Zhu, S. X., Lonning, P. E., Borresen-Dale, A. L., Brown, P. O., and Botstein, D. 2000. Molecular portraits of human breast tumours. *Nature* 406: 747–52.

Poland, C. A., Duffin, R., Kinloch, I., Maynard, A., Wallace, W. A., Seaton, A., Stone, V., Brown, S., Macnee, W., and Donaldson, K. 2008. Carbon nanotubes introduced into the abdominal cavity of mice show asbestos-like pathogenicity in a pilot study. *Nat Nanotechnol* 3: 423–28.

Porter, D., Sriram, K., Wolfarth, M., Jefferson, A., Schwegler-Berry, D., Andrew, M., and Castranova, V. 2008. A biocompatible medium for nanoparticle dispersion. *Nanotoxicology* 2: 144–54.

Porter, D. W., Hubbs, A. F., Mercer, R. R., Wu, N., Wolfarth, M. G., Sriram, K., Leonard, S., Battelli, L., Schwegler-Berry, D., Friend, S., Andrew, M., Chen, B. T., Tsuruoka, S., Endo, M., and Castranova, V. 2010. Mouse pulmonary dose- and time course-responses induced by exposure to multi-walled carbon nanotubes. *Toxicology* 269: 136–47.

Powell, C. L., Kosyk, O., Ross, P. K., Schoonhoven, R., Boysen, G., Swenberg, J. A., Heinloth, A. N., Boorman, G. A., Cunningham, M. L., Paules, R. S., and Rusyn, I. 2006. Phenotypic anchoring of acetaminophen-induced oxidative stress with gene expression profiles in rat liver. *Toxicol. Sci.* 93: 213–22.

Ryman-Rasmussen, J. P., Cesta, M. F., Brody, A. R., Shipley-Phillips, J. K., Everitt, J. I., Tewksbury, E. W., Moss, O. R., Wong, B. A., Dodd, D. E., Andersen, M. E., and Bonner, J. C. 2009. Inhaled carbon nanotubes reach the subpleural tissue in mice. *Nat. Nanotechnol.* 4: 747–51.

Sakai, S., Ono, M., Nishio, T., Kawarada, Y., Nagashima, A., and Toyoshima, S. 2003. Lung cancer associated with diffuse pulmonary fibrosis: CT-pathologic correlation. *J. Thorac. Imaging* 18: 67–71.

Sargent, L. M., Reynolds, S. H., and Castranova, V. 2010. Potential pulmonary effects of engineered carbon nanotubes: in vitro genotoxic effects. *Nanotoxicology* 4: 396–408.

Sargent, L. M., Reynolds, S. H., Hubbs, A. F., Benkovic, S. A., Lowry, D. T., Kashon, M. L., Siergrist, K. T., Mustovich, J., Sturgeon, J. L., Burker, K. L., and Dinu, C. Z. 2011. Understanding carbon nanotubes genotoxicity. *Toxicologist* 120: A59.

Scesnaite, A., Jarmalaite, S., Mutanen, P., Anttila, S., Nyberg, F., Benhamou, S., Boffetta, P., and Husgafvel-Pursiainen, K. 2012. Similar DNA methylation pattern in

lung tumours from smokers and never-smokers with second-hand tobacco smoke exposure. *Mutagenesis* 27: 423–29.

Selamat, S. A., Galler, J. S., Joshi, A. D., Fyfe, M. N., Campan, M., Siegmund, K. D., Kerr, K. M., and Laird-Offringa, I. A. 2011. DNA methylation changes in atypical adenomatous hyperplasia, adenocarcinoma in situ, and lung adenocarcinoma. *PLoS One* 6: e21443.

Shen, R. R., and Hahn, W. C. 2011. Emerging roles for the non-canonical IKKs in cancer. *Oncogene* 30: 631–41.

Shi, L., Campbell, G., Jones, W. D., Campagne, F., Wen, Z., Walker, S. J., Su, Z., Chu, T. M., Goodsaid, F. M., Pusztai, L., Shaughnessy, J. D., Jr., Oberthuer, A., Thomas, R. S., Paules, R. S., Fielden, M., Barlogie, B., Chen, W., Du, P., Fischer, M., Furlanello, C., Gallas, B. D., Ge, X., Megherbi, D. B., Symmans, W. F., Wang, M. D., Zhang, J., Bitter, H., Brors, B., Bushel, P. R., Bylesjo, M., Chen, M., Cheng, J., Chou, J., Davison, T. S., Delorenzi, M., Deng, Y., Devanarayan, V., Dix, D. J., Dopazo, J., Dorff, K. C., Elloumi, F., Fan, J., Fan, S., Fan, X., Fang, H., Gonzaludo, N., Hess, K. R., Hong, H., Huan, J., Irizarry, R. A., Judson, R., Juraeva, D., Lababidi, S., Lambert, C. G., Li, L., Li, Y., Li, Z., Lin, S. M., Liu, G., Lobenhofer, E. K., Luo, J., Luo, W., McCall, M. N., Nikolsky, Y., Pennello, G. A., Perkins, R. G., Philip, R., Popovici, V., Price, N. D., Qian, F., Scherer, A., Shi, T., Shi, W., Sung, J., Thierry-Mieg, D., Thierry-Mieg, J., Thodima, V., Trygg, J., Vishnuvajjala, L., Wang, S. J., Wu, J., Wu, Y., Xie, Q., Yousef, W. A., Zhang, L., Zhang, X., Zhong, S., Zhou, Y., Zhu, S., Arasappan, D., Bao, W., Lucas, A. B., Berthold, F., Brennan, R. J., Buness, A., Catalano, J. G., Chang, C., Chen, R., Cheng, Y., Cui, J., Czika, W., Demichelis, F., Deng, X., Dosymbekov, D., Eils, R., Feng, Y., Fostel, J., Fulmer-Smentek, S., Fuscoe, J. C., Gatto, L., Ge, W., Goldstein, D. R., Guo, L., Halbert, D. N., Han, J., Harris, S. C., Hatzis, C., Herman, D., Huang, J., Jensen, R. V., Jiang, R., Johnson, C. D., Jurman, G., Kahlert, Y., Khuder, S. A., Kohl, M., Li, J., Li, M., Li, Q. Z., Li, S., Liu, J., Liu, Y., Liu, Z., Meng, L., Madera, M., Martinez-Murillo, F., Medina, I., Meehan, J., Miclaus, K., Moffitt, R. A., Montaner, D., Mukherjee, P., Mulligan, G. J., Neville, P., Nikolskaya, T., Ning, B., Page, G. P., Parker, J., Parry, R. M., Peng, X., Peterson, R. L., Phan, J. H., Quanz, B., Ren, Y., Riccadonna, S., Roter, A. H., Samuelson, F. W., Schumacher, M. M., Shambaugh, J. D., Shi, Q., Shippy, R., Si, S., Smalter, A., Sotiriou, C., Soukup, M., Staedtler, F., Steiner, G., Stokes, T. H., Sun, Q., Tan, P. Y., Tang, R., Tezak, Z., Thorn, B., Tsyganova, M., Turpaz, Y., Vega, S. C., Visintainer, R., von Frese, J., Wang, C., Wang, E., Wang, J., Wang, W., Westermann, F., Willey, J. C., Woods, M., Wu, S., Xiao, N., Xu, J., Xu, L., Yang, L., Zeng, X., Zhang, M., Zhao, C., Puri, R. K., Scherf, U., Tong, W., and Wolfinger, R. D. 2010. The MicroArray Quality Control (MAQC)-II study of common practices for the development and validation of microarray-based predictive models. *Nat. Biotechnol.* 28: 827–38.

Shiels, M. S., Albanes, D., Virtamo, J., and Engels, E. A. 2011. Increased risk of lung cancer in men with tuberculosis in the alpha-tocopherol, Beta-carotene cancer prevention study. *Cancer Epidemiol. Biomarkers Prev.* 20: 672–78.

Shih, M. C., Chen, J. Y., Wu, Y. C., Jan, Y. H., Yang, B. M., Lu, P. J., Cheng, H. C., Huang, M. S., Yang, C. J., Hsiao, M., and Lai, J. M. 2012. TOPK/PBK promotes cell migration via modulation of the PI3K/PTEN/AKT pathway and is associated with poor prognosis in lung cancer. *Oncogene* 31: 2389–400

Shukla, A., Gulumian, M., Hei, T. K., Kamp, D., Rahman, Q., and Mossman, B. T. 2003. Multiple roles of oxidants in the pathogenesis of asbestos-induced diseases. *Free Radical Biol. Med.* 34: 1117–29.

Shvedova, A. A., Kapralov, A. A., Feng, W. H., Kisin, E. R., Murray, A. R., Mercer, R. R., St Croix, C. M., Lang, M. A., Watkins, S. C., Konduru, N. V., Allen, B. L., Conroy, J., Kotchey, G. P., Mohamed, B. M., Meade, A. D., Volkov, Y., Star, A., Fadeel, B., and Kagan, V. E. 2012. Impaired clearance and enhanced

pulmonary inflammatory/fibrotic response to carbon nanotubes in myeloperoxidase-deficient mice. *PLoS One* 7: e30923.

Shvedova, A. A., Kisin, E. R., Mercer, R., Murray, A. R., Johnson, V. J., Potapovich, A. I., Tyurina, Y. Y., Gorelik, O., Arepalli, S., Schwegler-Berry, D., Hubbs, A. F., Antonini, J., Evans, D. E., Ku, B. K., Ramsey, D., Maynard, A., Kagan, V. E., Castranova, V., and Baron, P. 2005. Unusual inflammatory and fibrogenic pulmonary responses to single-walled carbon nanotubes in mice. *Am. J. Physiol. Lung Cell. Mol. Physiol.* 289: L698–708.

Sorlie, T., Tibshirani, R., Parker, J., Hastie, T., Marron, J. S., Nobel, A., Deng, S., Johnsen, H., Pesich, R., Geisler, S., Demeter, J., Perou, C. M., Lonning, P. E., Brown, P. O., Borresen-Dale, A. L., and Botstein, D. 2003. Repeated observation of breast tumor subtypes in independent gene expression data sets. *Proc. Natl. Acad. Sci. USA* 100: 8418–23.

Sotiriou, C., Neo, S. Y., McShane, L. M., Korn, E. L., Long, P. M., Jazaeri, A., Martiat, P., Fox, S. B., Harris, A. L., and Liu, E. T. 2003. Breast cancer classification and prognosis based on gene expression profiles from a population-based study. *Proc. Natl. Acad. Sci. USA* 100: 10393–98.

Spira, A., Beane, J. E., Shah, V., Steiling, K., Liu, G., Schembri, F., Gilman, S., Dumas, Y. M., Calner, P., Sebastiani, P., Sridhar, S., Beamis, J., Lamb, C., Anderson, T., Gerry, N., Keane, J., Lenburg, M. E., and Brody, J. S. 2007. Airway epithelial gene expression in the diagnostic evaluation of smokers with suspect lung cancer. *Nat. Med.* 13: 361–66.

Stanton, M. F., Layard, M., Tegeris, A., Miller, E., May, M., Morgan, E., and Smith, A. 1981. Relation of particle dimension to carcinogenicity in amphibole asbestoses and other fibrous minerals. *J Natl Cancer Inst* 67: 965–75.

Strickert, M. 2007. Correlation-based data representation. *Similar. Cluster Appl. Med. Biol. Ser. Dagstuhl Seminar Proc.*, 1–16.

Tabet, L., Bussy, C., Amara, N., Setyan, A., Grodet, A., Rossi, M. J., Pairon, J. C., Boczkowski, J., and Lanone, S. 2009. Adverse effects of industrial multiwalled carbon nanotubes on human pulmonary cells. *J. Toxicol. Environ. Health A* 72: 60–73.

Takagi, A., Hirose, A., Nishimura, T., Fukumori, N., Ogata, A., Ohashi, N., Kitajima, S., and Kanno, J. 2008. Induction of mesothelioma in p53+/– mouse by intraperitoneal application of multi-wall carbon nanotube. *J. Toxicol. Sci.* 33: 105–116.

Takita, M., Arisaka, K., Kajita, T., Kifune, T., Koshiba, M., Miyano, K., Nakahata, M., Oyama, Y., Sato, N., Suda, T., Suzuki, A., Takahashi, K., and Totsuka, Y. 1986. Search for neutron–antineutron oscillation in ^{16}O nuclei. *Phys. Rev. D Part Fields* 34: 902–4.

Vallyathan, V., Green, F., Ducatman, B., and Schulte, P. 1998. Roles of epidemiology, pathology, molecular biology, and biomarkers in the investigation of occupational lung cancer. *J. Toxicol. Environ. Health B* 1: 91–116.

Van 't Veer, L. J., Dai, H., van de Vijver, M. J., He, Y. D., Hart, A. A., Mao, M., Peterse, H. L., van der Kooy, K., Marton, M. J., Witteveen, A. T., Schreiber, G. J., Kerkhoven, R. M., Roberts, C., Linsley, P. S., Bernards, R., and Friend, S. H. 2002. Gene expression profiling predicts clinical outcome of breast cancer. *Nature* 415: 530–36.

van de Vijver, M. J., He, Y. D., van 't Veer, L. J., Dai, H., Hart, A. A., Voskuil, D. W., Schreiber, G. J., Peterse, J. L., Roberts, C., Marton, M. J., Parrish, M., Atsma, D., Witteveen, A., Glas, A., Delahaye, L., van der Velde, T., Bartelink, H., Rodenhuis, S., Rutgers, E. T., Friend, S. H., and Bernards, R. 2002. A gene-expression signature as a predictor of survival in breast cancer. *N. Engl. J. Med.* 347: 1999–2009.

Van Dyke, A. L., Cote, M. L., Wenzlaff, A. S., Chen, W., Abrams, J., Land, S., Giroux, C. N., and Schwartz, A. G. 2009. Cytokine and cytokine receptor single-nucleotide polymorphisms predict risk for non-small cell lung cancer among women. *Cancer Epidemiol. Biomarkers Prev.* 18: 1829–40.

Vancheri, C., Failla, M., Crimi, N., and Raghu, G. 2010. Idiopathic pulmonary fibrosis: a

disease with similarities and links to cancer biology. *Eur. Respir. J.* 35: 496–504.

Vandenbroucke, R.E., Dejonckheere, E., and Libert, C. 2011. A therapeutic role for matrix metalloproteinase inhibitors in lung diseases? *Eur. Respir. J.* 38: 1200–14.

Vasiljeva, O., Papazoglou, A., Kruger, A., Brodoefel, H., Korovin, M., Deussing, J., Augustin, N., Nielsen, B. S., Almholt, K., Bogyo, M., Peters, C., and Reinheckel, T. 2006. Tumor cell-derived and macrophage-derived cathepsin B promotes progression and lung metastasis of mammary cancer. *Cancer Res.* 66: 5242–50.

Vaslet, C. A., Messier, N. J., and Kane, A. B. 2002. Accelerated progression of asbestos-induced mesotheliomas in heterozygous p53+/– mice. *Toxicol. Sci.* 68: 331–38.

Wan, Y. W., Sabbagh, E., Raese, R., Qian, Y., Luo, D., Denvir, J., Vallyathan, V., Castranova, V., and Guo, N. L. 2010. Hybrid models identified a 12-gene signature for lung cancer prognosis and chemoresponse prediction. *PLoS One* 5: e12222.

Wang, L., Castranova, V., Mishra, A., Chen, B., Mercer, R. R., Schwegler-Berry, D., and Rojanasakul, Y. 2010a. Dispersion of single-walled carbon nanotubes by a natural lung surfactant for pulmonary in vitro and in vivo toxicity studies. *Part. Fibre Toxicol.* 7: 31.

Wang, L., Luanpitpong, S., Castranova, V., Tse, W., Lu, Y., Pongrakhananon, V., and Rojanasakul, Y. 2011. Carbon nanotubes induce malignant transformation and tumorigenesis of human lung epithelial cells. *Nano Lett* 11: 2796–803.

Wang, X., Xia, T., Ntim, S. A., Ji, Z., George, S., Meng, H., Zhang, H.,Castranova, V., Mitra, S., and Nel, A. E. 2010b. Quantitative techniques for assessing and controlling the dispersion and biological effects of multiwalled carbon nanotubes in mammalian tissue culture cells. *ACS Nano* 4: 7241–52.

Wheeler, T. A., Porter, D. O., Archer, D., and Mullinix, B. G. 2008. Effect of fumigation on rotylenchulus reniformis population density through subsurface drip irrigation located every other furrow. *J. Nematol.* 40: 210–216.

Wikman, H., Ruosaari, S., Nymark, P., Sarhadi, V.K., Saharinen, J., Vanhala, E., Karjalainen, A., Hollmen, J., Knuutila, S., and Anttila, S. 2007. Gene expression and copy number profiling suggests the importance of allelic imbalance in 19p in asbestos-associated lung cancer. *Oncogene* 26: 4730–37.

Witten I. H. 2005. *Data mining: Practical machine learning tools and techniques* (2nd ed.). San Francisco, CA: Morgan Kaufmann.

Yu, Y. Y., Pinsky, P. F., Caporaso, N. E., Chatterjee, N., Baumgarten, M., Langenberg, P., Furuno, J. P., Lan, Q., and Engels, E. A. 2008. Lung cancer risk following detection of pulmonary scarring by chest radiography in the prostate, lung, colorectal, and ovarian cancer screening trial. *Arch. Intern. Med.* 168: 2326–32; discussion 2332.

Zhao, J., and Castranova, V. 2011. Toxicology of nanomaterials used in nanomedicine. *J. Toxicol. Environ. Health B Crit. Rev.* 14: 593–632.

Zhu, L., Chang, D.W., Dai, L., and Hong, Y. 2007. DNA damage induced by multiwalled carbon nanotubes in mouse embryonic stem cells. *Nano Lett.* 7: 3592–97.